J Mol Med
DOI 10.1007/s00109-014-1235-1

JMolMed

ORIGINAL ARTICLE

NNC 55-0396, a T-type Ca^{2+} channel inhibitor, inhibits angiogenesis via suppression of hypoxia-inducible factor-1α signal transduction

Ki Hyun Kim · Dongyoung Kim · Ju Yeol Park · Hye Jin Jung · Yong-Hee Cho · Hyoung Kyu Kim · Jin Han · Kang-Yell Choi · Ho Jeong Kwon

Received: 25 May 2014 / Revised: 8 November 2014 / Accepted: 14 November 2014

Abstract
Mitochondrial respiration is required for hypoxia-inducible factor (HIF)-1α stabilization, which is important for tumor cell survival, proliferation, and angiogenesis. Herein, small molecules that inhibit HIF-1α protein stability by targeting mitochondrial energy production were screened using the Library of Pharmacologically Active Compounds and cell growth assay in galactose or glucose medium. NNC 55-0396, a T-type Ca^{2+} channel inhibitor, was selected as a hit from among 1,280 small molecules. NNC 55-0396 suppressed mitochondrial reactive oxygen species-mediated HIF-1α expression as well as stabilization by inhibiting protein synthesis in a dose-dependent manner. NNC 55-0396 inhibited tumor-induced angiogenesis in vitro and in vivo by suppressing HIF-1α stability. Moreover, NNC 55-0396 significantly suppressed glioblastoma tumor growth in a xenograft model. Thus, NNC 55-0396, a small molecule targeting T-type Ca^{2+} channel, was identified by the systemic cell-based assay and was shown to have antiangiogenic activity via the suppression of HIF-1α signal transduction. These results provide new insights into the biological network between ion channel and HIF-1α signal transduction.

Key message
- HIF-1α overexpression has been demonstrated in hypoxic cancer cells.
- NNC 55-0396, a T-type Ca^{2+} channel inhibitor, inhibited HIF-1α expression via both proteasomal degradation and protein synthesis pathways.
- T-type Ca^{2+} channel inhibitors block angiogenesis by suppressing HIF-1α stability and synthesis.
- NNC 55-0396 could be a potential therapeutic drug candidate for cancer treatment.

Keywords Mitochondria · NNC 55-0396 · T-type Ca^{2+} channel · HIF-1α signal transduction · Angiogenesis

K. H. Kim · D. Kim · J. Y. Park · Y.-H. Cho · K.-Y. Choi · H. J. Kwon
Department of Biotechnology, Translational Research Center for Protein Function Control, College of Life Science and Biotechnology, Yonsei University, Seoul 120-749, South Korea

H. J. Jung
Department of Pharmaceutical Engineering, University of Sun Moon, Chungnam 330-150, South Korea

H. K. Kim · J. Han
Department of Physiology, Cardiovascular and Metabolic Disease Center, Inje University, Busan 614-749, South Korea

H. J. Kwon
Department of Internal Medicine, College of Medicine, Yonsei University, Seoul 120-752, South Korea

H. J. Kwon (✉)
Chemical Genomics National Research Laboratory, Department of Biotechnology, College of Life Science and Biotechnology, Yonsei University, 50 Yonsei-ro, Seodaemun-gu, Seoul 120-749, South Korea
e-mail: kwonhj@yonsei.ac.kr

Introduction

Hypoxia-inducible factor (HIF)-1 is an oxygen-sensitive transcription factor implicated in cancer biology, including the process of angiogenesis [1, 2]. HIF-1 consists of an oxygen-regulated subunit HIF-1α and a constitutively expressed subunit HIF-1β. The stability of the HIF-1α subunit is regulated by post-translational modifications, such as hydroxylation and ubiquitination under hypoxic conditions [3]. In addition to hypoxic conditions, HIF-1α is also regulated by cytokines, growth factors, and other signaling molecules, such as insulin, interleukin-1, tumor necrosis factor-alpha, mitogen-activated

Published online: 04 December 2014

protein kinase, or PI3K in an oxygen-independent manner [4–7]. The pivotal role of HIF-1α in cancer progression sheds light on this transcription factor as a potential target protein for cancer treatment.

Small molecules have often functioned as powerful probes for exploring biological questions [8]. For instance, FK506, an immunosuppressive agent, binds to FK506-binding protein (FKBP) and taxol binds to microtubules for their respective biological activity [9, 10]. Likewise, acriflavine was discovered as an inhibitor of HIF-1 dimerization, resulting in suppression of tumor growth and vascularization [11]. Terpestacin, a natural antiangiogenic small molecule, binds to mitochondrial ubiquinol-cytochrome c reductase binding protein (UQCRB) for its antiangiogenic activity, which revealed the role of UQCRB in angiogenesis and mitochondrial reactive oxygen species (ROS) signaling [12]. This binding of small molecules to their target proteins has helped to provide new insights into functions of the target proteins and finally aided drug development.

Due to the role of HIF-1α in cancer development and other diseases related to oxygen-sensitivity, new small molecules that can suppress HIF-1α activity are promising candidates for development of new therapeutic strategies. Targeting mitochondrial function in terms of reducing mitochondrial ROS has been reported to affect HIF-1α protein stability under hypoxic conditions [12–14]. Accordingly, small molecules that inhibit HIF-1α by targeting mitochondria were screened using the Library of Pharmacologically Active Compounds (LOPAC) and cell growth assay in galactose or glucose medium. LOPAC, a collection of 1,280 pharmacologically active compounds, is often utilized in drug discovery research for successful identification of new small molecules in biological assays of interest [15, 16]. Subsequently, suppression of cell growth in galactose medium by such small molecules is an indication of the inhibition of mitochondrial function [17]. Using this cell-based screening system, NNC 55-0396 was identified as a potent small molecule that suppressed HIF-1α signal transduction. NNC 55-0396 was found to regulate hypoxia-induced HIF-1α protein stability not only via proteasomal degradation but also via protein synthesis. Moreover, it also significantly suppressed tumor-induced angiogenesis and tumor growth in mouse xenograft assays. Collectively, these results identify a new chemical probe that can modulate HIF-1α signal transduction by targeting the T-type Ca^{2+} channel.

Materials and methods

Materials

LOPAC and NNC 55-0396 were purchased from Sigma Aldrich (St. Louis, MO, USA). Kurtoxin was kindly provided by Dr. JaeIl Kim, GIST, Korea. Anti-HIF-1α and PECAM-1 were purchased from BD Biosciences (San Jose, CA, USA). Anti-CACNA1H, vascular endothelial growth factor (VEGF), and tubulin were purchased from Santa Cruz Biotechnology (Dallas, TX, USA), Abcam (Cambridge, UK), and Millipore (Bilerica, MA, USA), respectively. Anti-HIF-1β and CACN A1C were purchased from NOVUS Biologicals (Littleton, CO, USA). Anti-hydroxy-HIF-1α, mammalian target of rapamycin (mTOR), phospho-mTOR, p70S6K, and phospho-p70S6Kwere purchased from Cell Signaling Technology (Beverly, MA, USA).

Cell culture and hypoxic conditions

Early passages (passages 4–8) of human umbilical vein endothelial cells (HUVECs) were grown in endothelial growth medium (EGM)-2 (Lonza, Walkersville, MD, USA) supplemented with 10 % fetal bovine serum (FBS) (Invitrogen, Grand Island, NY, USA). HepG2 (human liver carcinoma) and U87-MG (human glioblastoma) cells were grown in Dulbecco's modified Eagle's medium (DMEM) and MEM (Invitrogen) containing 10 % FBS. All cells were maintained at 37 °C in a humidified 5 % CO_2 incubator. For hypoxic conditions, small molecules were pretreated 1 h, and cells were incubated for indicated time with 5 % CO_2 and 1 % O_2 balanced with N_2 in an anaerobic chamber after overnight serum starvation (Forma, Marietta, OH, USA).

Cell growth assay in the glucose or galactose medium

For the cell growth assay, HepG2 cells were maintained in high-glucose medium and then transferred to glucose-free medium supplemented with 10 mM galactose and incubated for at least 1 week. HepG2 cells were then seeded in 96-well plates at a concentration of 2000 cells/well. LOPAC compounds were treated individually to the cells to identify compounds that inhibited cell proliferation. Cells were grown for 72 h and growth was analyzed using the 3-(4,5-dimehylthiazol-2-yl)-2,5-diphenyl tetrazolium bromide (MTT, Sigma-Aldrich) colorimetric assay [18].

T-type Ca^{2+} channel RNA interference and reverse transcriptase–polymerase chain reaction analysis

Human CACNA1H-specific small interfering RNA (siRNA) (siCACNA1H) was synthesized by Genolution Pharmaceuticals, Inc. (Seoul, South Korea). The sense and antisense sequences of this siRNA were 5′-GUG CGA CGC AAG UAC AAC UUU-3′ and 5′-AGU UGU ACU UGC GUC GCA CUU-3′, respectively. For depletion of CACNA1H mRNA, HepG2 were transfected with either scrambled, negative, or CACNA1H siRNA using Lipofectamine 2000 transfection reagent (Invitrogen) according to the manufacturer's instructions. CACNA1H and CANCA1C mRNA were

validated by reverse transcriptase–polymerase chain reaction analysis using primers specific for CACNA1H (sense, 5′-TCG AGG AGG ACT TCC ACA AG-3′; antisense, 5′-TGC ATC CAG GAA TGG TGA G-3′) and CACNA1C (sense, 5′-GCC GAA GAC ATC GAT CCT GA-3′; antisense, 5′-GAA AAT CAC CAG CCA GTA GAA GA-3′).

Measurement of mitochondrial ROS

Mitochondrial ROS levels were measured using a MitoSOX™ Red mitochondrial superoxide indicator (Invitrogen). Once in the mitochondria, the MitoSOX™ Red reagent is oxidized by superoxide and emits red fluorescence. After incubation with MitoSOX™ Red (5 μM) for 10 min, the cells were washed with washing buffer, and the fluorescent images were obtained using a microscope (IX71, Olympus), and the fluorescence intensity was quantified by Image J software (National Institute of Health, Bethesda, MD, USA).

In vitro tumor cell-induced angiogenesis assay

Tumor cell-induced capillary tube formation and chemoinvasion by HUVECs were assessed using tumor cell conditioned medium (CM). HepG2 cells were plated in 12-well culture plates and then serum-starved overnight. Serum-starved HepG2 were pretreated with NNC 55-0396 and incubated under hypoxic conditions. CM was collected after 16 h and concentrated by ultra-centrifugation. Subsequently, in vitro angiogenesis assays using CM were performed as described previously [12]. Invaded cells and tube formations were observed under a microscope and photographed at ×100 magnification.

Western blot analysis

Cell lysates were separated by 10 % sodium dodecyl sulfate–polyacrylamide gel electrophoresis (SDS-PAGE), and the separated proteins were transferred to polyvinylidenedifluoride (PVDF) membranes (Millipore) using standard electroblotting procedures Blots were blocked and immunolabeled overnight at 4 °C with primary antibodies against HIF-1α, hydroxy-HIF-1α, HIF-1β, CACNA1C, CACNA1H, tubulin, phospho-mTOR, mTOR, phospho-p70S6K, and p70S6K. Immunolabeling was visualized using an ECL kit (Amersham, Buckinghamshire, UK) according to the manufacturer's instructions.

Measurement of VEGF by ELISA

The VEGF concentration in media from NNC 55-0396-treated cells for 16 h was determined using a VEGF Immunoassay kit (R&D systems, Minneapolis, MN, USA) according to the manufacturer's instructions. The results were expressed as concentration of VEGF relative to the total amount of VEGF from each well.

Chorioallantoic membrane assay

The chorioallantoic membrane (CAM) assay was performed as described previously [14]. Fertilized chick eggs were kept in a humidified incubator at 37 °C for 4 days. About 4–5 mL of egg albumin was removed with a hypodermic needle, allowing the CAM and yolk sac to drop away from the shell membrane. On day 5, CM with or without NNC 55-0396 were loaded on thermanox coverslip (NUNC, Rochester, NY, USA) and were applied to the CAM surface. Two days later, 1 mL of Intralipose (Greencross Co, Korea) was injected beneath the CAM. The membrane was observed under a microscope and photographed at ×20 magnification.

In vivo mouse tumor xenograft assay

Four-week-old female BALB/c-nu/nu mice were purchased from Narabio (Seoul, Korea). Animal care and experiments were carried out according to the guidelines of the Korean Food and Drug Administration. Protocols were reviewed and approved by the Institutional Review Board of Severance Hospital, Yonsei University, College of Medicine (09-013). After acclimatization for 1 week, 3×10^7 U87-MG cells in 100 μL phosphate-buffered saline (PBS)/Matrigel (1:1) were subcutaneously injected into the dorsal flank of athymic nude mice. When the mean size of tumors was between 80 and 120 mm^3, NNC 55-0396 was administered intraperitoneally to the mice at doses of 10 and 20 mg/kg, every 2 days. Tumor volume and body weight of mice were measured every 4 days. Tumor volumes were measured with Vernier calipers, using the formula $\pi/6\times\text{length}\times\text{width}\times\text{height}$. Twenty days after treatment, the mice were killed, and the tumors were excised, weighed, and fixed in paraformaldehyde for further analysis [19].

Immunohistochemistry

Xenograft tumors were fixed overnight in 4 % paraformaldehyde. Paraffin sections (4 μM thick) were deparaffinized and rehydrated. The sections were boiled in 10 mM citrate buffer (pH 6.0) and blocked in 3.4 % hydrogen peroxide for 15 min. The slides were incubated overnight at 4 °C with the following dilutions of primary antibodies: anti-HIF-1α and VEGF. After washing with PBS, the specimens were incubated with biotinylated secondary antibody for 1 h and streptavidin peroxidase at room temperature for 30 min. Finally, the specimens were visualized using a diaminobenzidine reagent kit (Vector Laboratories, Burlingame, CA, USA). The immunostained sections were counterstained with hematoxylin. Cryosections (10 μM thick) were incubated overnight at 4 °C with PECAM-1 primary antibody. After washing with PBS, the specimens were incubated with Alexa Fluor 647 anti-rat secondary antibody for 1 h.

Statistical analysis

Results are expressed as the mean±standard error (SE). Student's *t* test was used to determine statistical significance between the control and test groups. A $p<0.05$ was considered statistically significant.

Results

Small molecule screening for inhibitors that suppressed mitochondrion-mediated HIF-1α protein stability

To identify new bioactive small molecules that affect mitochondrial function, we used small molecules from LOPAC and the cell growth assay with glucose or galactose medium [17]. The effect of small molecules on cell growth was analyzed by relative cell growth in glucose versus galactose medium (Fig. 1a, left), and the highest inhibition rates 100 compounds were assigned a $S_{glu/gal}$ score, defined as the log ratio of cell growth in glucose divided by that in galactose (Fig. 1a, right). The top 100 compounds that inhibited cell growth in galactose medium by possibly modulating mitochondrial function showed positive $S_{glu/gal}$ scores. Since regulation of mitochondrion-mediated HIF-1α protein stability during hypoxia is important for tumor progression, the effect of hits on HIF-1α protein stability was evaluated. From 100 compounds, two hits were identified, which are T-type Ca^{2+} channel blockers. These two compounds (NNC 55-0396 and mibefradil) suppressed hypoxia-induced HIF-1α protein stability with no effect on HIF-1β stability (Fig. 1b). Notably, mibefradil is a Ca^{2+} channel antagonist that inhibits both T-type and high-voltage-activated Ca^{2+} channels, whereas NNC 55-0396, a derivative of mibefradil, has a selective inhibitory effect on T-type Ca^{2+} channel (Fig. 1c, d) [20]. Accordingly, the studies that followed focused on the activity of NNC 55-0396 on HIF-1α protein stability.

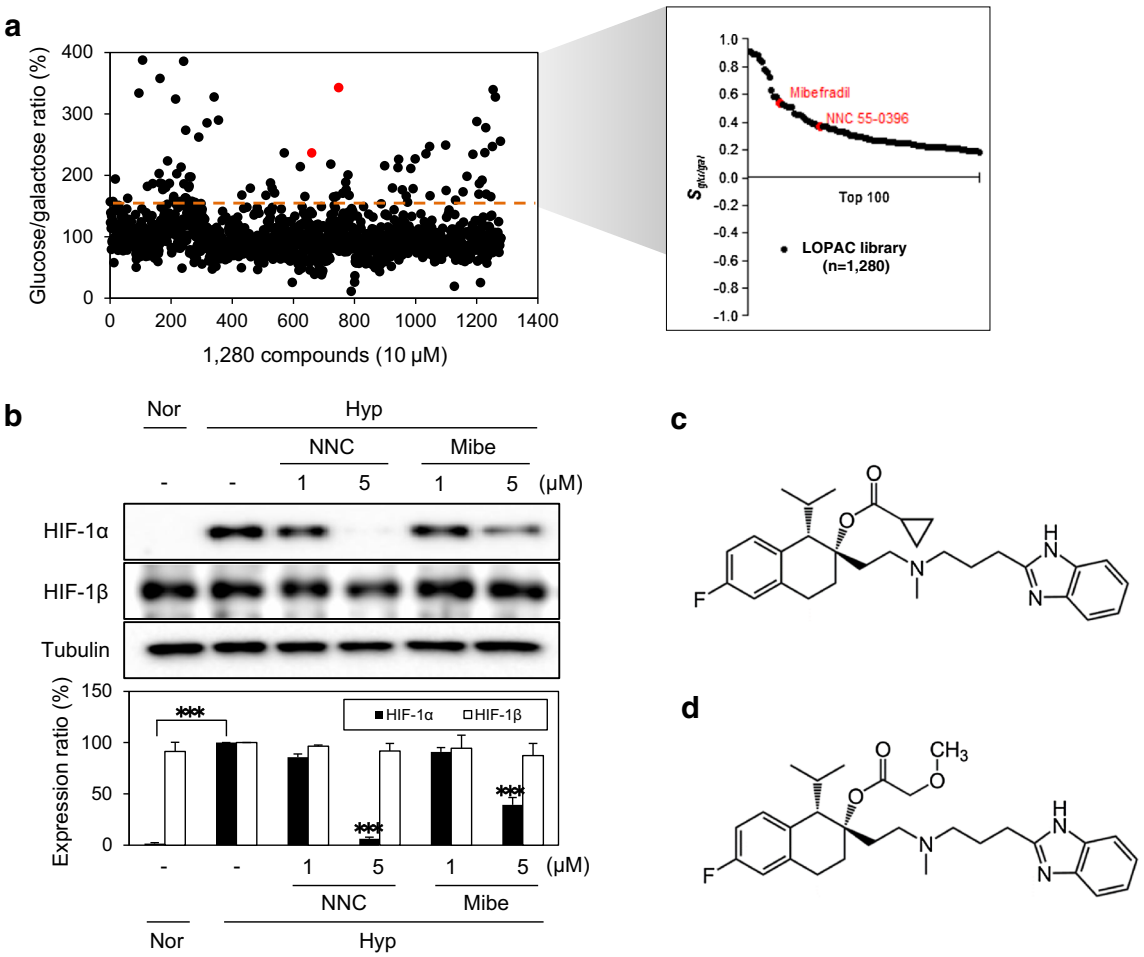

Fig. 1 Screening for mitochondrion-mediated angiogenesis inhibitors with LOPAC. **a** Results from cell growth assay in galactose versus glucose media. In the case of 100 compounds, inhibition of cell growth in glucose medium was 150 % higher than that in galactose medium (*left*). The logarithm of the cell growth in glucose versus galactose provides a summary statistic ($S_{glu/gal}$) for each compound. The highest inhibition rates 100 compounds plotted by $S_{glu/gal}$ (*right*). **b** Effects of T-type Ca^{2+} channel inhibitors on HIF-1α and HIF-1β protein stability. Tubulin was used as an internal control. *Nor* normoxia, *Hyp* hypoxia, *NNC* NNC55-0396, *Mibe* mibefradil. ***$p<0.001$. Each value represents the mean±SE from three independent experiments. **c** Structure of NNC55-0396. **d** Structure of mibefradil

T-type Ca^{2+} channel specifically regulates HIF-1α protein stability

The functional role of Ca^{2+} signaling in HIF-1α signal transduction has been recently highlighted. Recent reports demonstrated that Ca^{2+} signaling stimulates translation of HIF-α during hypoxia, and the activation of HIF-1α transcriptional activity by Ca^{2+} signal was evaluated [21, 22]. However, the mechanism of Ca^{2+} channel-mediated regulation of HIF-1α protein stability during hypoxia remains unclear. To address this, effects of Ca^{2+} channel modulators on HIF-1α protein stability were investigated in this study. First, HepG2 cells were treated with T- and L-type Ca^{2+} channel inhibitors under conditions of hypoxia. Notably, HIF-1α protein stability was selectively inhibited by the T-type Ca^{2+} channel inhibitors NNC 55-0396 (NNC), mibefradil (Mibe), and kurtoxin (Kur) (Fig. 2a). Next, the cells were treated with T-type (CACNA1H) and L-type (CACNA1C) Ca^{2+} channel antibodies. T-type Ca^{2+} channel antibody inhibited HIF-1α protein stability (Fig. 2b). Finally, the role of T-type Ca^{2+} channel in HIF-1α protein stability was investigated via genetic knockdown using T-type Ca^{2+} channel siRNA. As shown in Fig. 2c, knockdown of T-type Ca^{2+} channel suppressed hypoxia-induced HIF-1α protein stability. In addition, an increase in the expression level of T-type Ca^{2+} channel subunit was induced by hypoxia, whereas the L-type Ca^{2+} channel subunit was not affected (Fig. 2d) [23]. This increase in T-type Ca^{2+} channel levels indicates that it has a functional role in cell response to hypoxia. Collectively, these results demonstrate that HIF-1α protein stability is selectively regulated by T-type Ca^{2+} channel activities during hypoxia.

NNC 55-0396 affected HIF-1α protein stability through proteasomal degradation and HIF-1α protein synthesis

Effect of NNC 55-0396 on HIF-1α protein stability was examined in detail, since NNC 55-0396 did not affect HIF-1α mRNA levels (Fig. 3a). The mitochondrion is a major site of cellular ROS generation during hypoxia, and the induction of mitochondrial ROS has been reported as a key factor for hypoxia-induced stabilization of HIF-1α [24, 25]. First, the

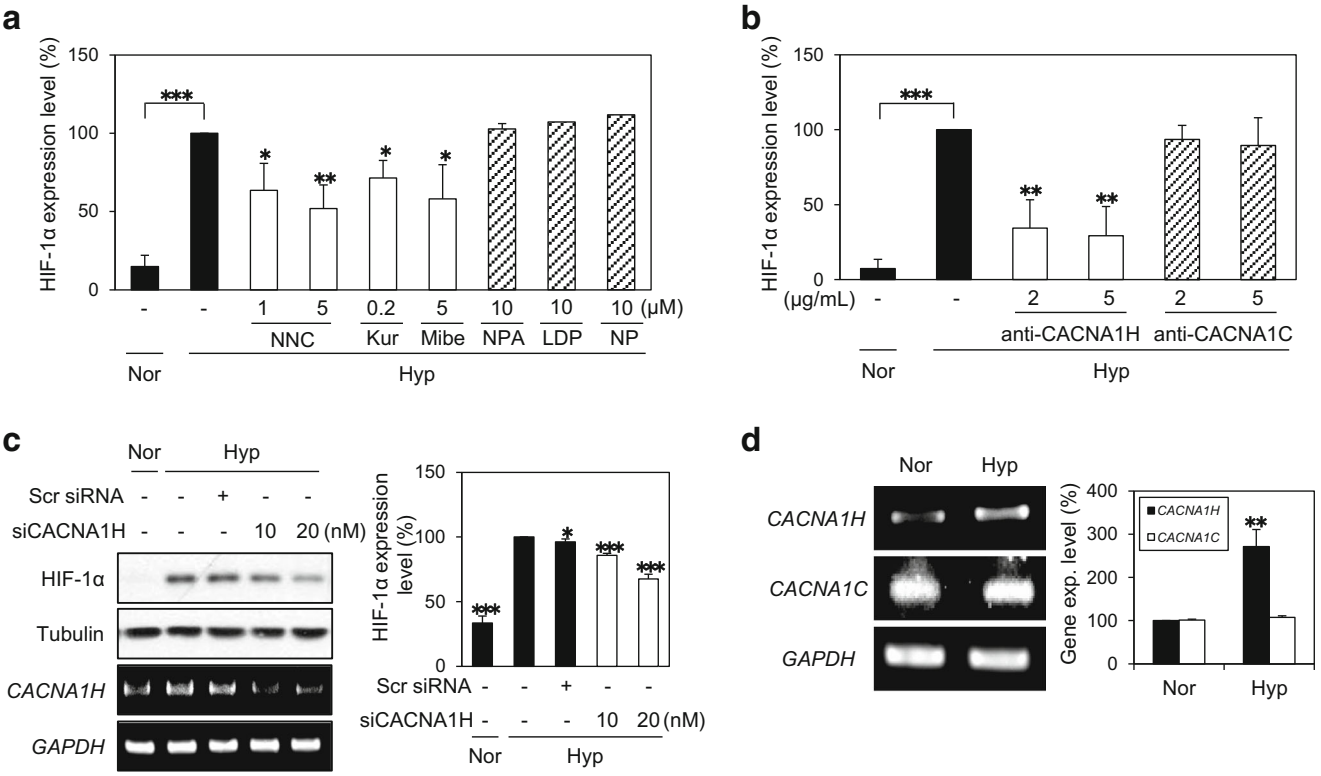

Fig. 2 T-type Ca^{2+} channel specifically regulate HIF-1α protein stability. **a** Effects of Ca^{2+} channel inhibitors on HIF-1α protein stability. Serum-starved HepG2 were pretreated with inhibitors and then incubated in a hypoxia chamber for 4 h. *Kur* kurtoxin, *NPA* nemadipine A, *LDP* lercanidipine,*NP* nimodipine. *p<0.05; **p<0.01; ***p<0.001. Each value represents the mean±SE from three independent experiments. **b** Effects of Ca^{2+} channel antibodies on HIF-1α protein stability. Serum-starved HepG2 cells were pretreated with CACNA1H (T-type Ca^{2+} channel) and CACNA1C (L-type Ca^{2+} channel) antibodies and incubated in a hypoxia chamber for 4 h. **p<0.01; ***p<0.001. Each value represents the mean±SE from three independent experiments. **c** Effect of T-type Ca^{2+} channel knockdown on HIF-1α protein stability. HepG2 cells were transfected with either scrambled siRNA or CACN A1H siRNA (siCACNA1H). *p<0.05, ***p<0.001. Each value represents the mean±SE from three independent experiments. **d** Effect of Ca^{2+} channel subunit expression level under hypoxic conditions. **p<0.01. Each value represents the mean±SE from three independent experiments

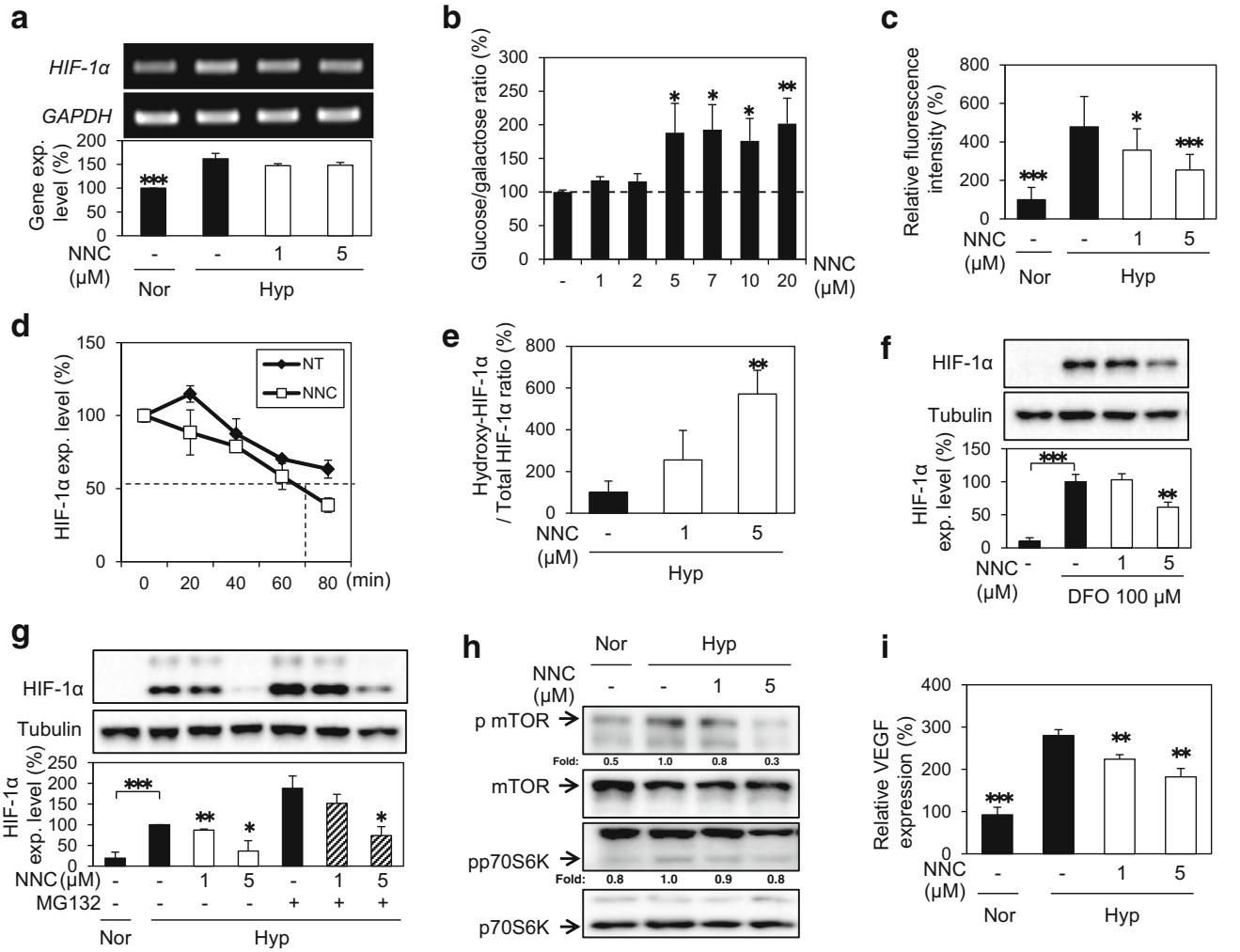

Fig. 3 Suppression of mitochondrial ROS-mediated HIF-1α expression. **a** Effect of NNC 55-0396 on HIF-1α mRNA levels. HepG2 cells were pretreated with NNC 55-0396 (1–5 μM) for 1 h and then exposed to 1 % O_2 for 12 h. ***p<0.001. Each value represents the mean±SE from three independent experiments. **b** Cell growth ratio in galactose versus glucose media with or without 1–20 μM NNC 55-0396 was measured using MTT assay at 72 h. *p<0.05; **p<0.01. Each value represents the mean±SE from three independent experiments. **c** Mitochondrial ROS levels were determined by MitoSOX staining in HepG2 cells incubated under hypoxic conditions for 1 h with or without 1 and 5 μM NNC 55-0396. MitoSOX staining images were quantified using Image J software.*p<0.05; ***p<0.001. Each value represents the mean±SE from three independent experiments. **d** Effect of NNC 55-0396 on HIF-1α stabilization. HepG2 cells were pretreated with NNC 55-0396 (1 μM) for 1 h and incubated under hypoxic conditions for 2 h. HIF-1α half-life was measured with cycloheximide (CHX, 30 μg/mL) for the indicated time periods under hypoxic conditions to block all de novo protein synthesis. *NT* non-treated cells under hypoxia, *NNC* NNC-treated cells under hypoxia. Each value represents the mean±SE from three independent experiments. **e** Effect of NNC 55-0396 on hydroxylation of HIF-1α protein. HepG2 cells were pretreated with NNC 55-0396 (1 and 5 μM) for 1 h and then incubated for 4 h. Hydroxyl-HIF-1α and total HIF-1α protein were detected by Western blot. **p<0.01; ***p<0.001. Each value represents the mean±SE from three independent experiments. **f** Detection of desferrioxamine (DFO)-induced HIF-1α protein stability. HepG2 cells were pretreated with NNC 55-0396 (1 and 5 μM) for 1 h and then incubated in the presence of 100 μM DFO for 4 h. **p<0.01; ***p<0.001. Each value represents the mean±SE from three independent experiments. **g** HIF-1α protein accumulates in response to proteasomal inhibition. HepG2 cells were exposed to MG132 (20 μM) for 2 h. *p<0.05; **p<0.01; ***p<0.001. Each value represents the mean±SE from three independent experiments. **h** Effects of NNC 55-0396 on HIF-1α synthesis signal transduction. HepG2 cells were pretreated with NNC 55-0396 (1 μM) for 1 h and then incubated under hypoxic conditions for 15 min. Protein levels were analyzed using Western blot analysis. The data shown are representative of three independent experiments. **i** Effects of NNC 55-0396 on VEGF expression level. HepG2 cells were pretreated with NNC 55-0396 (1 μM) for 1 h and then incubated under hypoxic conditions for 16 h. VEGF expression level on CM were analyzed using ELISA assay. **p<0.01; ***p<0.001. Each value represents the mean±SE from three independent experiments

inhibition of mitochondrial function by NNC 55-0396 was investigated using a cell growth assay in galactose medium. NNC 55-0396 exhibited stronger inhibitory effects on cell growth in galactose medium than in glucose (Fig. 3b). Next, the mitochondrial ROS levels in HepG2 cells were evaluated using MitoSOX, a red mitochondrial superoxide indicator. NNC 55-0396 was found to significantly suppress the generation of hypoxia-induced mitochondrial ROS (Fig. 3c). To

investigate whether NNC 55-0396 affects HIF-1α protein stability by suppressing mitochondrial ROS, HIF-1α half-life using cycloheximide (CHX) and hydroxyl-HIF-1α stability were examined. As shown in Fig. 3d, when HepG2 cells were pretreated with 1 μM NNC 55-0396, HIF-1α half-life decreased from >80 min to <70 min. NNC 55-0396 also increased the hydroxylation of HIF-1α that is related to VHL E3 ligase interaction (Fig. 3e). To further verify whether NNC 55-0396 inhibits HIF-1α protein stability by suppressing mitochondrial ROS generation, the effect of NNC 55-0396 on desferrioxamine (DFO)-induced accumulation of HIF-1α was investigated. DFO, an iron chelator that inhibits proline hydroxylase (PHD) function by binding free Fe^{2+}, does not require mitochondrial ROS [26]. Notably, NNC 55-0396 also inhibited the stabilization of HIF-1α with DFO treatment (Fig. 3f). The effect of NNC 55-0396 on HIF-1α protein synthesis using MG132 was evaluated. Treatment with NNC 55-0396 under hypoxia in the presence of MG132 exhibited a decrease in ubiquitinylated HIF-1α protein levels (Fig. 3g). NNC 55-0396 also repressed the phosphorylation of mTOR and p70S6K that modulate translation and synthesis of HIF-1α (Fig. 3h). In addition, NNC 55-0396 decreased the expression level of VEGF, one target of HIF-1α in Fig. 3i. Collectively, these results imply that NNC 55-0396 suppresses HIF-1α protein stability through both protein degradation and synthesis pathways.

NNC 55-0396 inhibits tumor-induced angiogenesis both in vitro and in vivo

Under hypoxic conditions, HIF-1α translocates into the nucleus with HIF-1β and activates the transcription of target genes, such as VEGF, which promotes angiogenesis [27]. Accordingly, the inhibitory activities of NNC 55-0396 on the tumor-induced angiogenic phenotypes of HUVECs were assessed in vitro and in vivo. First, a chemo-invasion assay was conducted on serum-starved HUVECs using tumor cell-CM with or without NNC 55-0396 treatment. NNC 55-0396

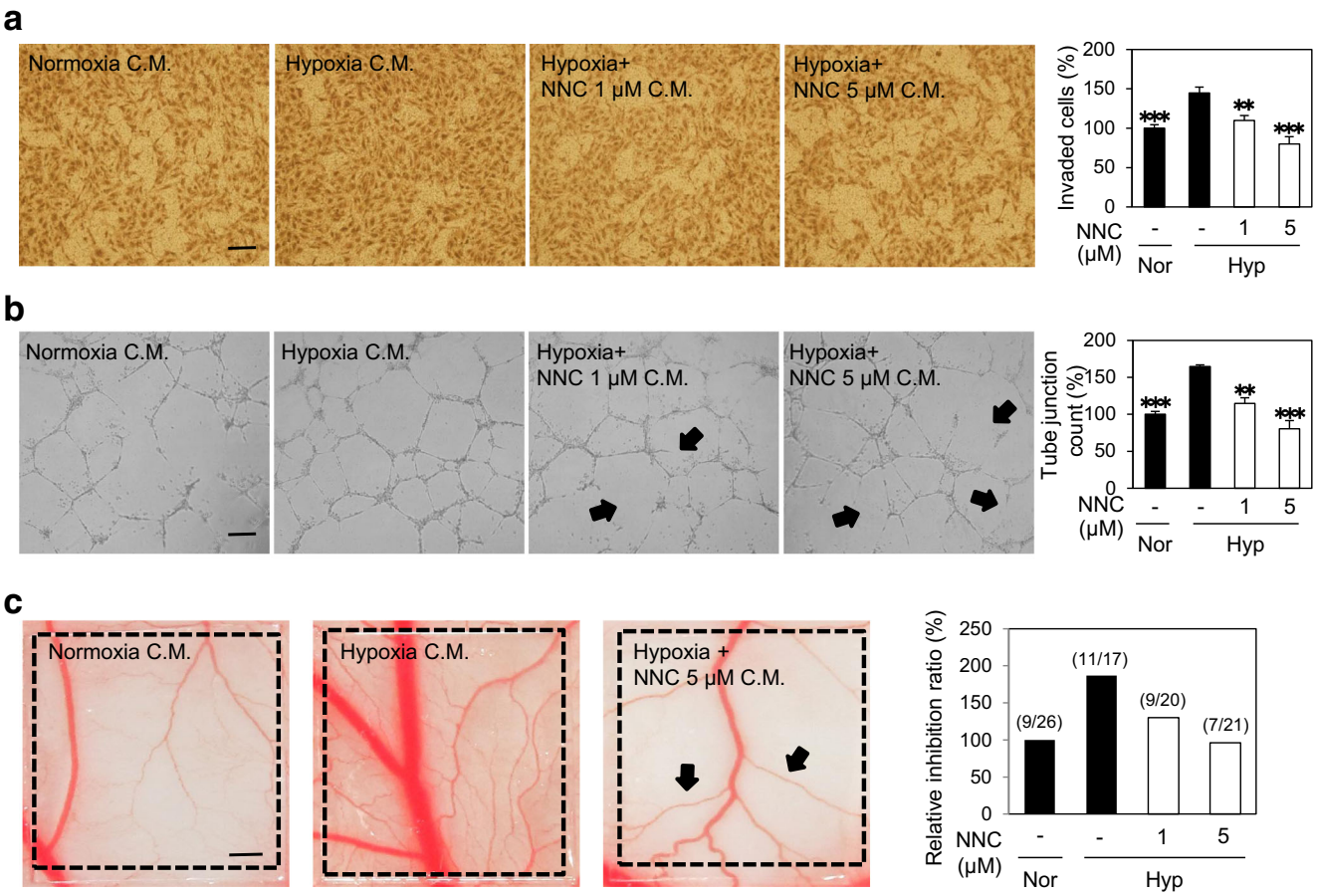

Fig. 4 Effect of NNC 55-0396 on tumor-induced angiogenesis. **a** Effect of NNC55-0396-treated CM on invasion by HUVECs. $^{**}p<0.01$; $^{***}p<0.001$. Each value represents the mean±SE from three independent experiments. Scale bar, 100 μm. **b** Inhibitory effect of NNC 55-0396-treated CM on tube formation by HUVECs. *Arrows* indicate broken tubes formed by tumor CM-induced HUVECs. $^{**}p<0.01$; $^{***}p<0.001$. Each value represents the mean±SE from three independent experiments. Scale bar, 100 μm. **c** Antiangiogenesis activity of NNC 55-0396 in vivo. CAM was treated with CM derived from HepG2 cells cultured with or without NNC 55-0396. *Arrows* indicate inhibition of neovascularization by CAM. The data shown are representative of three independent experiments and calculations were based on the proportion of positive eggs relative to the total number of eggs tested (positive eggs/total eggs). Scale bar, 1 mm

inhibited tumor-induced tube formation by HUVECs in a dose-dependent manner (Fig. 4a). The effect of NNC 55-0396 on tumor-induced tube formation by HUVECs was investigated, and NNC 55-0396 showed inhibitory effects on tube formation with no cytotoxic effects (Fig. 4b). Next, the in vivo inhibitory effect of NNC 55-0396 on tumor-induced angiogenesis was also investigated using the chick embryo chorioallantoic membrane (CAM) assay. As shown Fig. 6c, hypoxia-induced CM-treated CAMs showed strong induction of new capillaries from the existing vascular network, whereas NNC 55-0396-treated CAMs showed weak angiogenic activity during CAM development without any sign of thrombosis or hemorrhage. Collectively, these data demonstrate that NNC 55-0396 potently inhibits in vitro and in vivo tumor-induced angiogenesis.

NNC 55-0396 inhibits tumor growth in a tumor xenograft mouse model

The antitumor effect of NNC 55-0396 was measured using a mouse tumor xenograft model. U87-MG cells (human glioblastoma), which are a highly lethal type of cancer cells that exhibit striking angiogenesis with elevated expression of VEGF, were used in this assay [28]. *BALB/c-nu/nu* mice were inoculated with 3×10^7 U87-MG cells, and the mice were intraperitoneally treated with either a vehicle or NNC 55-0396. The representative gross images of tumors are shown in Fig. 5a. NNC 55-0396 treatment (10 and 20 mg/kg) reduced both the volume (Fig. 5b) and weight (Fig. 5c) of xenograft tumors. In addition, NNC 55-0396 did not affect weight or induce liver toxicity in mice (data not shown). Immunohistochemical analysis was

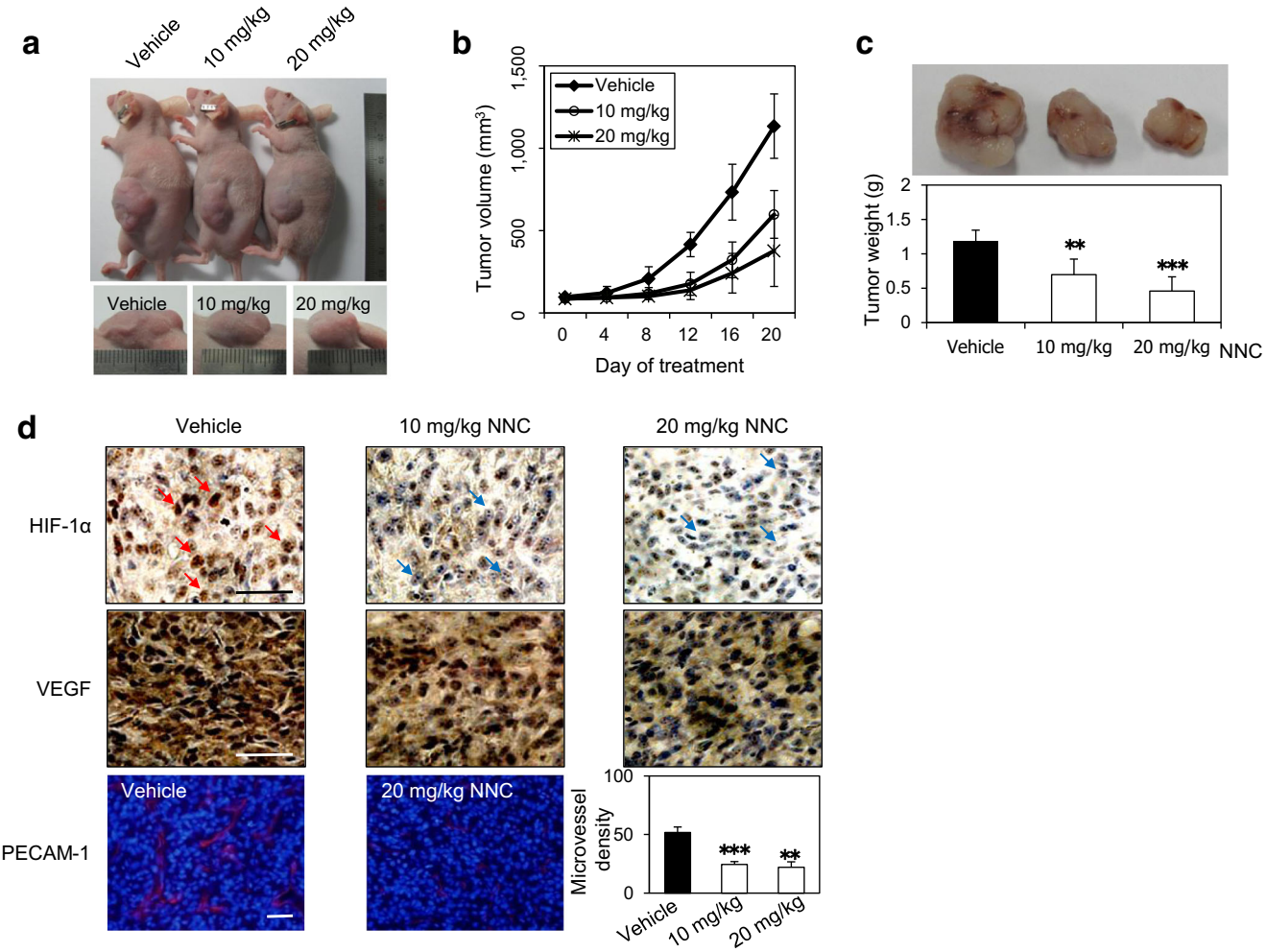

Fig. 5 Effect of NNC 55-0396 on xenograft tumors. **a** Five athymic nude mice bearing glioblastoma consisting of U87-MG cells were treated with vehicle or NNC 55-0396 (10 and 20 mg/kg). Gross images showing representative cases treated with NNC 55-0396. **b** Tumor volumes of three groups (n=5) after 20 days. **c** The weight of tumors obtained from mice treated with the vehicle or NNC 55-0396 was measured using an electronic balance. **d** Effect of NNC 55-0396 on the expression levels of HIF-1α, VEGF, and PECAM-1 in xenograft tumors. Paraformaldehyde-fixed paraffin sections and cryosections were incubated with HIF-1α, VEGF, and PECAM-1 antibodies. *Red arrows* indicate HIF-1α expression in the nucleus. *Blue arrows* indicate the inhibition of HIF-1α expression in the nucleus. Microvessel density was measured by counting the number of positive structures in three random fields. Original magnification of DAP staining images (HIF-1α and VEGF): ×400. Scale bar, 100 μm. Original magnification of fluorescence images (PECAM-1): ×200. Scale bar, 100 μm. **p<0.01; ***p<0.001

performed to confirm the effect of NNC 55-0396 on xenograft tumors. HIF-1α, VEGF, and PECAM-1 expression levels in the xenograft tumors were significantly reduced by NNC 55-0396 treatment (Fig. 5d).

Discussion

HIF-1α is a key transcription factor for angiogenesis, which is a pivotal step in cancer development [1, 2, 29]. Therefore, blocking HIF-1α activity is a promising strategy for cancer therapy. HIF-1α activation during hypoxia is a multistep process involving HIF-1α protein stability, α and β subunit dimerization, nuclear translocation, binding to HRE elements, and the formation of active transcriptional complexes [27]. In the present study, a new antiangiogenic small molecule, NNC 55-0396, which suppressed HIF-1α protein stability by inhibiting both protein degradation and synthesis, was identified.

Recent studies indicate that Ca^{2+} plays a key role in the hypoxic cellular response and an increase of Ca^{2+} level was observed in endothelial cells during hypoxia [30, 31]. In particular, T-type Ca^{2+} channel activity increases with chronic hypoxia [23, 32, 33]. In addition, Ca^{2+} activation by phospholipase C (PLC) and mTOR pathways contribute to the stabilization of HIF-1α protein by intermittent hypoxia [34]. However, a correlation between Ca^{2+} channel and HIF-1α protein stability during hypoxia is not clear. Although cilnidipine, an L-type Ca^{2+} channel inhibitor, has been shown to inhibit HIF-1α protein stability, its effect did not depend on blocking of the L-type Ca^{2+} channel [35]. Our study demonstrated that T-type Ca^{2+} channel inhibitor, NNC 55-0396 inhibited angiogenesis by suppressing HIF-1α protein stability. This observation is consistent with in vitro and in vivo angiogenesis assays as well as in vivo mouse xenograft model assays (Fig. 6).

In the present study, T-type Ca^{2+} channel inhibitors (NNC 55-0396, mibefradil, and kurtoxin) suppressed hypoxia-induced HIF-1α protein stability. NNC 55-0396 showed not only inhibitory activities with respect to mitochondrial-mediated HIF-1α protein stability but also inhibition of HIF-1α protein stability by blocking protein synthesis de novo. Therefore, NNC 55-0396 effects on HIF-1α were attributed to inhibition of proteasomal degradation and protein synthesis. However, NNC 55-0396 and kurtoxin did not show the same effects on cell growth in galactose or glucose medium. Kurtoxin did not inhibit cell growth in galactose medium at doses that affected HIF-1α protein stability (unpublished result). These data suggest that the mitochondrion-mediated inhibitory activities might be intrinsic characteristics of NNC 55-0396. To elucidate the effects on mitochondria by NNC 55-0396, mitochondrial oxygen consumption rate (OCR) and

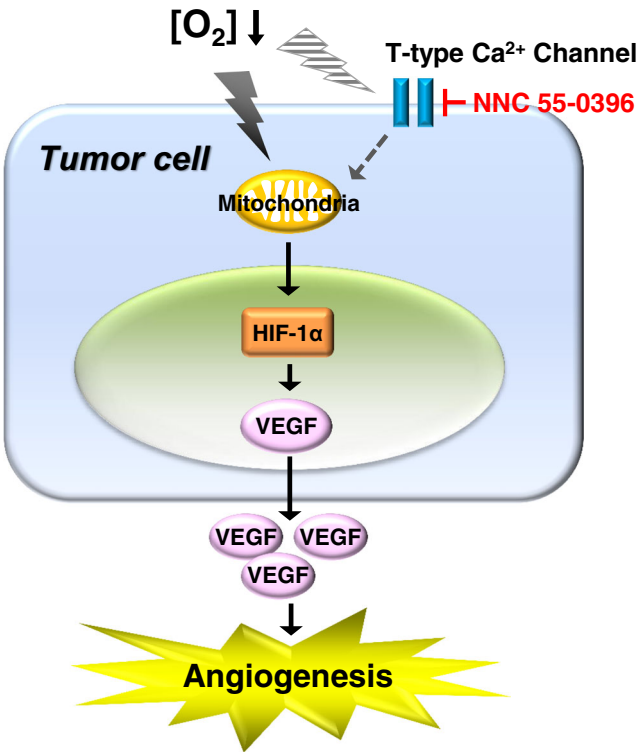

Fig. 6 Role of T-type Ca^{2+} channel in HIF-1α signal transduction. The model suggests that T-type Ca^{2+} channel is one of the mediators of HIF-1α stabilization in tumor cells and its small molecule blocker, NNC 55-0396, inhibits mitochondrial ROS-mediated HIF-1α signal transduction and tumor-induced angiogenesis

ATP levels on mouse myoblast C2C12 were measured, and NNC 55-0396 showed the inhibitory activities on mitochondrial OCR and ATP levels (unpublished result). Therefore, the further studies on the mitochondrial function on HepG2 are necessary to assess mode of action of NNC 55-0396. The mechanism by which T-type Ca^{2+} channel inhibition causes mitochondrion-mediated suppression of HIF-1α protein stability remains elusive, but this study newly demonstrated that T-type Ca^{2+} channel inhibition by pharmacologically and genetically is responsible for decreased HIF-1α protein stability and inhibition of angiogenesis. Moreover, NNC 55-0396 inhibited tumor-induced angiogenesis in vitro and in vivo by suppressing HIF-1α stability. It is noteworthy that NNC 55-0396 significantly decreased highly malignant and HIF-1α-dependent glioblastoma tumor growth in a xenograft model.

Collectively, NNC 55-0396 is newly identified as a novel angiogenesis inhibitor by phenotypic screening and biological validation methods. Furthermore, these results provide new insights into the mechanisms of HIF-1α protein stability that involve T-type Ca^{2+} channel inhibition. These findings suggest that the regulation of the T-type Ca^{2+} channel could be a new therapeutic strategy for improving cancer treatment efficacy.

Acknowledgments This study was partly supported by grants from the National Research Foundation of Korea funded by the Korean government (MSIP; 2010-0017984, 2012M3A9D1054520), the Translational Research Center for Protein Function Control, KRF (2009-0083522), the Next-Generation BioGreen 21 Program (No. PJ0079772012), Rural Development Administration, National R&D Program, Ministry of Health &Welfare (0620360-1), and the Brain Korea 21 Plus Project, Republic of Korea.

Conflict of interest There is no conflict of interest to disclose.

References

1. Wang GL, Semenza GL (1995) Purification and characterization of hypoxia-inducible factor 1. J Biol Chem 270:1230–1237
2. Mazure NM, Brahimi-Horn MC, Berta MA, Benizri E, Bilton RL, Dayan F, Ginouves A, Berra E, Pouyssegur J (2004) HIF-1: master and commander of the hypoxic world. A pharmacological approach to its regulation by siRNAs. Biochem Pharmacol 68:971–980
3. Masson N, Ratcliffe PJ (2003) HIF prolyl and asparaginyl hydroxylases in the biological response to intracellular O(2) levels. J Cell Sci 116:3041–3049
4. Zelzer E, Levy Y, Kahana C, Shilo BZ, Rubinstein M, Cohen B (1998) Insulin induces transcription of target genes through the hypoxia-inducible factor HIF-1alpha/ARNT. EMBO J 17:5085–5094
5. Thornton RD, Lane P, Borghaei RC, Pease EA, Caro J, Mochan E (2000) Interleukin 1 induces hypoxia-inducible factor 1 in human gingival and synovial fibroblasts. Biochem J 350(Pt 1):307–312
6. Kuo HP, Lee DF, Xia W, Wei Y, Hung MC (2009) TNFalpha induces HIF-1alpha expression through activation of IKKbeta. Biochem Biophys Res Commun 389:640–644
7. Li J, Davidson G, Huang Y, Jiang BH, Shi X, Costa M, Huang C (2004) Nickel compounds act through phosphatidylinositol-3-kinase/Akt-dependent, p70(S6k)-independent pathway to induce hypoxia inducible factor transactivation and Cap43 expression in mouse epidermal Cl41 cells. Cancer Res 64:94–101
8. Kwon HJ (2006) Discovery of new small molecules and targets towards angiogenesis via chemical genomics approach. Curr Drug Targets 7:397–405
9. Harding MW, Galat A, Uehling DE, Schreiber SL (1989) A receptor for the immunosuppressant FK506 is a cis-trans peptidyl-prolyl isomerase. Nature 341:758–760
10. Schiff PB, Fant J, Horwitz SB (1979) Promotion of microtubule assembly in vitro by taxol. Nature 277:665–667
11. Lee K, Zhang H, Qian DZ, Rey S, Liu JO, Semenza GL (2009) Acriflavine inhibits HIF-1 dimerization, tumor growth, and vascularization. Proc Natl Acad Sci U S A 106:17910–17915
12. Jung HJ, Shim JS, Lee J, Song YM, Park KC, Choi SH, Kim ND, Yoon JH, Mungai PT, Schumacker PT et al (2010) Terpestacin inhibits tumor angiogenesis by targeting UQCRB of mitochondrial complex III and suppressing hypoxia-induced reactive oxygen species production and cellular oxygen sensing. J Biol Chem 285:11584–11595
13. Chandel NS, Maltepe E, Goldwasser E, Mathieu CE, Simon MC, Schumacker PT (1998) Mitochondrial reactive oxygen species trigger hypoxia-induced transcription. Proc Natl Acad Sci U S A 95:11715–11720
14. Kim KH, Park JY, Jung HJ, Kwon HJ (2011) Identification and biological activities of a new antiangiogenic small molecule that suppresses mitochondrial reactive oxygen species. Biochem Biophys Res Commun 404:541–545
15. Lai TS, Liu Y, Tucker T, Daniel KR, Sane DC, Toone E, Toone E, Burke JR, Strittmatter WJ, Greenberg CS (2008) Identification of chemical inhibitors to human tissue transglutaminase by screening existing drug libraries. Chem Biol 15:969–978
16. Schulz MM, Reisen F, Zgraggen S, Fischer S, Yuen D, Kang GJ, Kang GJ, Chen L, Schneider G, Detmar M (2012) Phenotype-based high-content chemical library screening identifies statins as inhibitors of in vivo lymphangiogenesis. Proc Natl Acad Sci U S A 109:E2665–E2674
17. Lin X, David CA, Donnelly JB, Michaelides M, Chandel NS, Huang X, Warrior U, Weinberg F, Tormos KV, Fesik SW et al (2008) A chemical genomics screen highlights the essential role of mitochondria in HIF-1 regulation. Proc Natl Acad Sci U S A 105:174–179
18. Gohil VM, Sheth SA, Nilsson R, Wojtovich AP, Lee JH, Perocchi F, Chen W, Clish CB, Ayata C, Brookes PS et al (2010) Nutrient-sensitized screening for drugs that shift energy metabolism from mitochondrial respiration to glycolysis. Nat Biotechnol 28:249–255
19. Yoon J, Koo KH, Choi KY (2011) MEK1/2 inhibitors AS703026 and AZD6244 may be potential therapies for KRAS mutated colorectal cancer that is resistant to EGFR monoclonal antibody therapy. Cancer Res 71:445–453
20. Huang L, Keyser BM, Tagmose TM, Hansen JB, Taylor JT, Zhuang H, Zhang M, Ragsdale DS, Li M (2004) NNC 55-0396 [(1S,2S)-2-(2-(N-[(3-benzimidazol-2-yl)propyl]-N-methylamino)ethyl)-6-fluoro-1,2,3,4-tetrahydro-1-isopropyl-2-naphtyl cyclopropanecarboxylate dihydrochloride]: a new selective inhibitor of T-type calcium channels. J Pharmacol Exp Ther 309:193–199
21. Hui AS, Bauer AL, Striet JB, Schnell PO, Czyzyk-Krzeska MF (2006) Calcium signaling stimulates translation of HIF-alpha during hypoxia. FASEB J: Off Publ Fed Am Socr Exp Biol 20:466–475
22. Yuan G, Nanduri J, Bhasker CR, Semenza GL, Prabhakar NR (2005) Ca^{2+}/calmodulin kinase-dependent activation of hypoxia inducible factor 1 transcriptional activity in cells subjected to intermittent hypoxia. J Biol Chem 280:4321–4328
23. Del Toro R, Levitsky KL, Lopez-Barneo J, Chiara MD (2003) Induction of T-type calcium channel gene expression by chronic hypoxia. J Biol Chem 278:22316–22324
24. Guzy RD, Hoyos B, Robin E, Chen H, Liu L, Mansfield KD, Simon MC, Hammerling U, Schumacker PT (2005) Mitochondrial complex III is required for hypoxia-induced ROS production and cellular oxygen sensing. Cell Metab 1:401–408
25. Vanden Hoek TL, Becker LB, Shao Z, Li C, Schumacker PT (1998) Reactive oxygen species released from mitochondria during brief hypoxia induce preconditioning in cardiomyocytes. J Biol Chem 273:18092–18098
26. Triantafyllou A, Liakos P, Tsakalof A, Georgatsou E, Simos G, Bonanou S (2006) Cobalt induces hypoxia-inducible factor-1alpha (HIF-1alpha) in HeLa cells by an iron-independent, but ROS-, PI-3 K- and MAPK-dependent mechanism. Free Radic Res 40:847–856
27. Forsythe JA, Jiang BH, Iyer NV, Agani F, Leung SW, Koos RD, Semenza GL (1996) Activation of vascular endothelial growth factor gene transcription by hypoxia-inducible factor 1. Mol Cell Biol 16:4604–4613
28. Plate KH, Breier G, Weich HA, Risau W (1992) Vascular endothelial growth-factor is a potential tumor angiogenesis factor in human gliomas invivo. Nature 359:845–848
29. Semenza GL (2013) Cancer-stromal cell interactions mediated by hypoxia-inducible factors promote angiogenesis, lymphangiogenesis, and metastasis. Oncogene 32:4057–4063
30. Arnould T, Michiels C, Alexandre I, Remacle J (1992) Effect of hypoxia upon intracellular calcium concentration of human endothelial cells. J Cell Physiol 152:215–221
31. Seta KA, Yuan Y, Spicer Z, Lu G, Bedard J, Ferguson TK, Pathrose P, Cole-Strauss A, Kaufhold A, Millhorn DE (2004) The role of calcium in hypoxia-induced signal transduction and gene expression. Cell Calcium 36:331–340

32. Levitsky KL, Lopez-Barneo J (2009) Developmental change of T-type Ca2+ channel expression and its role in rat chromaffin cell responsiveness to acute hypoxia. J Physiol 587:1917–1929
33. Wan J, Yamamura A, Zimnicka AM, Voiriot G, Smith KA, Tang H, Ayon RJ, Choudhury MS, Ko EA, Wang J et al (2013) Chronic hypoxia selectively enhances L- and T-type voltage-dependent Ca^{2+} channel activity in pulmonary artery by upregulating Cav1.2 and Cav3.2. Am J Physiol Lung Cell Mol Physiol 305:L154–L164
34. Yuan G, Nanduri J, Khan S, Semenza GL, Prabhakar NR (2008) Induction of HIF-1alpha expression by intermittent hypoxia: involvement of NADPH oxidase, Ca^{2+} signaling, prolyl hydroxylases, and mTOR. J Cell Physiol 217:674–685
35. Oda S, Oda T, Takabuchi S, Nishi K, Wakamatsu T, Tanaka T, Adachi T, Fukuda K, Nohara R, Hirota K (2009) The calcium channel blocker cilnidipine selectively suppresses hypoxia-inducible factor 1 activity in vascular cells. Eur J Pharmacol 606:130–136